

Nuclear Magnetic Resonance Measurements in Oil-Nitrogen Two-Phase Flow

G. J. Krüger and A. Birke

Joint Research Centre (Ispra) European Commission, 21020 Ispra (VA), Italy

Z. Naturforsch. **50a**, 845–851 (1995); received May 11, 1995

Herrn Prof. Werner Müller-Warmuth zum 65. Geburtstag gewidmet in Erinnerung an langjährige fruchtbare Zusammenarbeit

NMR measurements of the oil mass flow have been carried out in all-oil flow as well as in oil-nitrogen two-phase flow. For the calibration a simplified method was used which circumvents spin-lattice relaxation calculations due to the short polarization time of the protons at rather high flow velocities. With this method an overall accuracy of the oil-flow in oil-nitrogen two-phase flow of about $\pm 5\%$ was achieved.

Some proposals for an improvement of the NMR apparatus are made, which would render the evaluations simpler and more accurate.

Introduction

Most of the NMR work on flow has been devoted to relatively slow flow for applications to e.g. medicine [1]. In contrast to this we have proposed a new NMR method for fast and highly turbulent flow [2]. The aim of the present paper is the application of this method to measurements of oil-nitrogen two-phase flow. For the measurement we used heating oil AMOCO type 3/5 with dynamic viscosity between 20 and 35 cP and relative density 0.945. This liquid is much more viscous than water and has correspondingly shorter nuclear relaxation times, which influence the measurements and the evaluations.

Some General Considerations on NMR Two-Phase Flow Measurements

Our measurement arrangement is shown in Figure 1. The flow is downwards and consists either of oil or an oil-nitrogen mixture. Our NMR spectrometer is a computer-controlled BRUKER CXP spectrometer. It uses proton resonance and measures only the liquid flow. The magnet has a length of 40 cm in flow direction. Its resonance field B_0 of about 0.0939 T (corresponding to our proton resonance frequency of 4 MHz) serves also for the polarization of the spins. Under flow conditions the spins spend on average the

polarization time t_p in the magnetic field before they reach the measuring region of the RF coil in the center of the magnet. Hence the nuclear magnetization M parallel to B_0 has to be multiplied by a relaxation factor $1 - \exp(-t_p/T_1)$ with T_1 being the spin-lattice relaxation time.

In our RF coil the 8 kW transmitter can produce a magnetic RF field B_{RF} with amplitude $2B_1$ as usual. We use a Carr-Purcell-Gill-Meiboom pulse sequence [2–4]. This creates a spin-echo sequence, the envelope of which is, in the absence of flow, proportional to $\exp(-t/T_2)$ with the spin-spin relaxation time T_2 . If we have flow in addition, the spins originally tilted by the 90° pulse, which form the nuclear magnetization $m(t)$ in the direction transverse to the magnetic field B_0 , will leave the coil physically due to the flow. In this case the echo envelope decreases accordingly in an efflux curve EFC (t/T_E), where the characteristic time T_E is the efflux time [2]. After this time has elapsed, all the observable spins will have left the RF coil and no transverse magnetization can any longer be detected. Thus the transverse magnetization as measured by the echo envelope will have the form

$$m(t) = M_0 \cdot [1 - \exp(-t_p/T_1)] \cdot \text{EFC}(t/T_E) \cdot \exp(-t/T_2). \quad (1)$$

Here M_0 is the nuclear paramagnetic equilibrium magnetization

$$M_0 = \chi_0 B_0, \quad (2)$$

Reprint requests to Dr. G. J. Krüger, v. Cunardo 37, I-21039 Bedero Valcuvia (VA), Italy.

0932-0784 / 95 / 0900-0845 \$ 06.00 © – Verlag der Zeitschrift für Naturforschung, D-72027 Tübingen



Dieses Werk wurde im Jahr 2013 vom Verlag Zeitschrift für Naturforschung in Zusammenarbeit mit der Max-Planck-Gesellschaft zur Förderung der Wissenschaften e.V. digitalisiert und unter folgender Lizenz veröffentlicht: Creative Commons Namensnennung-Keine Bearbeitung 3.0 Deutschland Lizenz.

Zum 01.01.2015 ist eine Anpassung der Lizenzbedingungen (Entfall der Creative Commons Lizenzbedingung „Keine Bearbeitung“) beabsichtigt, um eine Nachnutzung auch im Rahmen zukünftiger wissenschaftlicher Nutzungsformen zu ermöglichen.

This work has been digitalized and published in 2013 by Verlag Zeitschrift für Naturforschung in cooperation with the Max Planck Society for the Advancement of Science under a Creative Commons Attribution-NoDerivs 3.0 Germany License.

On 01.01.2015 it is planned to change the License Conditions (the removal of the Creative Commons License condition “no derivative works”). This is to allow reuse in the area of future scientific usage.

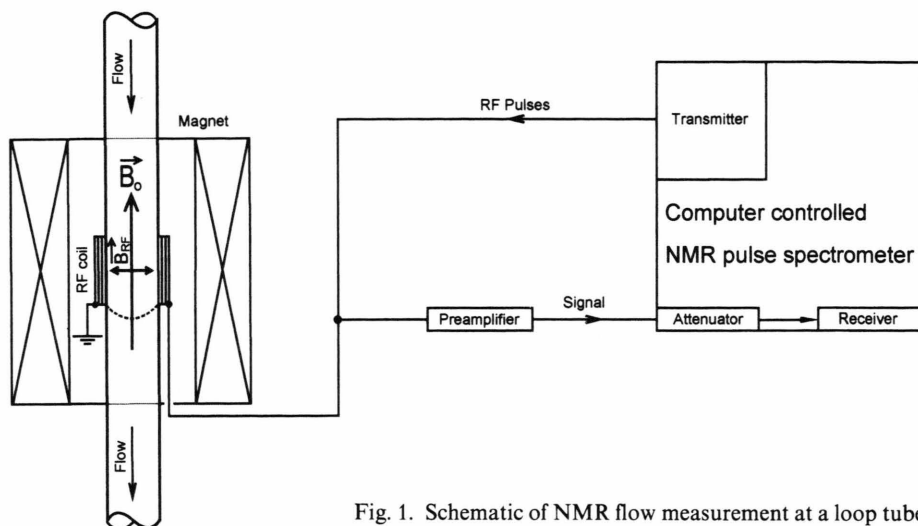


Fig. 1. Schematic of NMR flow measurement at a loop tube.

where

$$\chi_0 = N \gamma^2 \hbar^2 I(I+1)/(3kT) \quad (3)$$

is the static nuclear paramagnetic susceptibility. N is the number of spins I in the liquid per volume and γ the magnetogyroscopic ratio of the spins. These equations show that, at least in principle, we can obtain the liquid fraction from the magnetization M_0 , which is proportional to N . The average velocity can be evaluated from the time dependence of the efflux curve. The evaluation procedure has been outlined in [2]. It will be briefly described here:

At first we assumed idealized conditions with an homogeneous magnetic field B_1 inside the RF coil of length L_c in flow direction and zero field outside this coil. Thus the spins tilted by the 90° pulse form a cylinder of length L_c and the inner diameter of the loop tube. Further we assumed that all the spins exhibit exactly the same velocity v . Thus this whole cylinder of tagged spins will move downstream with this velocity after the 90° pulse. After time t it will have moved by the distance vt . If we neglect relaxation effects, the echo sequence will then decay as

$$m(t) = m_0(1 - vt/L_c) = m_0(1 - t/T_E). \quad (4)$$

This is a simple efflux curve with the efflux time $T_E = L_c/v$. After this time, the whole cylinder will have moved out of the RF coil and consequently the echo sequence will have decayed to zero. With a real RF coil we do not have such a nicely shaped B_1 field, and (4) will no more be valid. If we still assume the same

velocity for all the spins, we get

$$m(t) = m_0 \text{ISC}(t/T_E) \quad (5)$$

instead. The efflux curve is now an iso-speed curve ISC. This is a type of calibration efflux curve which depends on the geometry of the magnetic field. It must be determined experimentally for each specific coil arrangement. We got it by pulling a sealed piece of the loop tube filled with water through our RF coil. This coil is similar to a saddle coil, has as length of 10 cm and consists of six windings arranged round the flow tube in such a way as to obtain a sufficient homogeneity of the B_1 field over the inner cross-section of the tube [5].

In a real flow situation we have a velocity distribution. To each group of spins with velocity v_i and corresponding efflux time T_{Ei} we ascribe a partial magnetization m_{0i} at the end of the 90° pulse. These partial magnetizations form the velocity probability distribution. Each group of spins with velocity v_i has further an iso-speed curve $\text{ISC}(t/T_{Ei})$. The sum of all these iso-speed curves, weighted by the partial magnetizations, is then our measured efflux curve EFC. For the practical evaluation of such an efflux curve in an unknown flow situation we assume a set of N_v equally spaced efflux times T_{Ei} according to the time-scale of the EFC. N_v is the number of spin groups with corresponding velocities v_i . Then we calculate the partial magnetizations m_{0i} by an iterative computer fit of the sum of the iso-speed curves to the measured efflux

curve according to

$$m_0 \text{EFC}(t/\langle T_E \rangle) = \sum_{i=1}^{N_v} m_{0i} \text{ISC}(t/T_{Ei}). \quad (6)$$

Thus we obtain an average value of the magnetization immediately after the 90° pulse, which cannot be measured directly due to the receiver dead time after the 8 kW transmitter pulse

$$m_0 = \sum_{i=1}^{N_v} m_{0i} \quad (7)$$

and the average efflux time

$$\langle T_E \rangle = \sum_{i=1}^{N_v} m_{0i} T_{Ei} / m_0 \equiv T_E, \quad (8)$$

which we denote by T_E for the sake of simplicity. Finally we get the average flow velocity

$$\langle v \rangle \equiv v = L_{fe} / T_E \quad (9)$$

where L_{fe} is the effective length of the B_1 field, which must be determined by a calibration experiment with known velocity in all-liquid flow.

Application of NMR to Oil-Nitrogen Two-Phase Flow

We turn back to the test section of our liquid-gas test loop shown schematically in Figure 1. The inner diameter of the test section is 4.2 cm. The loop has a tank (about 3000 l) where the oil is stored. It can be used as a closed loop, where the oil is pumped through the test section and then back to the tank. In this way the loop is used for calibration measurements in all-oil flow. The oil mass flow is measured by a turbine directly behind the pump, where we have always all-oil flow. Downstream there is a mixing vessel where we inject nitrogen gas to obtain oil-nitrogen two-phase flow. The nitrogen flow is measured by an MKS type 558A mass flow meter before the mixing. In addition we measure the pressure and temperature at our measuring section as well as in the gas flow and the liquid flow before the mixing. These data allow a calculation of the liquid fraction $\varepsilon_{\text{loop}}$ from the loop input data as usual. For two-phase flow measurements the loop is open-ended and the oil-nitrogen mixture is discharged after the measurement. This is the only possibility to obtain constant fluid mixture conditions for the measurements, since recirculation would result in an increasing amount of nitrogen trapped in the oil.

The measurement is accomplished by measuring the echo maxima only. Each spin echo gives one measured value, and with these we obtain the echo envelope, which shows the decay of the transverse nuclear magnetization $m(t)$ and has the form

$$m(t) = A_0 \cdot \text{EFC}(t/T_E) \cdot \exp(-t/T_2) \\ = A_{00} \cdot AT \cdot \text{EFC}(t/T_E) \cdot \exp(-t/T_2). \quad (10)$$

Here A_0 is the measured signal amplitude immediately after the 90° pulse at the time $t=0$ and A_{00} is the same amplitude normalized to an attenuation of 0 db at our receiver attenuator with attenuation AT . This latter is necessary in order to compare measurements of different velocities and hence polarization times and amplitudes. Comparing (1) and (10) we find

$$A_{00} \propto M_0 [1 - \exp(-t_p/T_1)]. \quad (11)$$

In order to obtain the efflux curve, we must first correct our measured curve for T_2 effects. This can be done either by the known relaxation time T_2 , calculating $\exp(-t/T_2)$ for each echo and dividing the echo value by it. A better possibility, which we normally apply, is to stop the flow after the measurement, measure the echo envelope without flow at the same time scale as the flow measurement and then correct point by point of the latter by the corresponding points of the experimental T_2 correction curve. This method works also for liquid mixtures, whose components have different relaxation times T_2 . In this way we obtain the EFC without T_2 effects, and from this EFC we get the average efflux time $\langle T_E \rangle$ of the efflux time distribution as described above and in [2].

We assume pseudo-stationary flow conditions to such an extent that the average values of the amplitude A_{00} , efflux time T_E and velocity v remain constant over the whole time of the measurement including the polarization time t_p . Under this assumption, and using (9) we can state that

$$t_p \propto T_E \propto 1/v. \quad (12)$$

Expanding $1 - \exp(-t_p/T_1)$ in a power series up to the third power of t_p , we obtain from (11) and (12)

$$A_{00}/T_E = A_1 + A_2/v + A_3/v^2. \quad (13)$$

Now we perform a series of calibration measurements using liquid flow without gas at different velocities and hence different efflux times T_E and velocities v measured by the turbine meter. Then we do a least-squares fit of A_{00}/T_E versus v according to (13) and thus obtain

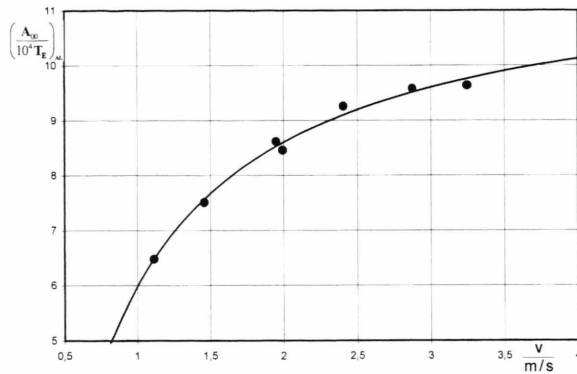


Fig. 2. Amplitude calibration $(A_{00}/T_E)_{AL}$ in arbitrary units vs. velocity v measured by turbine at all-oil flow.

the constants A_1 , A_2 , and A_3 . This is shown in Fig. 2, where we have plotted the measured values $(A_{00}/T_E)_{AL}$ in arbitrary units obtained at all-liquid flow versus the velocity v . The curve in the figure is the least-squares fit to the data. This ordinate becomes constant at high velocities. This is a great advantage against the direct dependence of the amplitude $A_{00}(v)$, which is varying much more with v . It is worthwhile mentioning that, of course, A_2 must be negative and

$$A_1 > |A_2| > A_3. \quad (14)$$

If (14) is fulfilled, the calibration procedure is reasonable. In the case of Fig. 2 the constants divided by 10^4 were $A_1 = 11.780$, $A_2 = -6.908$, and $A_3 = 1.106$.

With this preparation we make two-phase flow measurements and obtain, of course, for each measurement a two-phase value $(A_{00}/T_E)_{2p}$ at a certain value of v . These two-phase flows exhibit normally high velocities. So we are nearly in the constant part of (13) and can calculate $(A_{00}/T_E)_{AL}$, which we would obtain at all-liquid flow at the same velocity using our fitted constants A_1 , A_2 , and A_3 . The liquid fraction ε_1 is then obtained in a straightforward manner by the ratio

$$\varepsilon_1 \equiv \varepsilon_{NMR} = \frac{(A_{00}/T_E)_{2p}}{(A_{00}/T_E)_{AL}}. \quad (15)$$

This approach avoids the determination of the polarization length and T_1 correction calculations, which cannot be done reasonably in a flow situation as given in our experiments. It works also for long relaxation times T_1 , and thus we do not need the addition of paramagnetic species in order to shorten T_1 . This method is a technical approach in order to obtain

meaningful values of ε_1 with an accuracy which is sufficient for technical purposes.

From our all-liquid flow measurements we can obtain the mean velocity v in our measuring section using the liquid mass flow measurement by the turbine at the loop before the liquid gas mixing device. This velocity can be used to get the effective length L_{fe} of the B_1 field in the RF coil by (9). This length depends slightly on the velocity because of the change in the turbulence and of the influence of this turbulence on the T_E measurement. This T_E dependence is weak. We therefore make an ansatz as (13) and write

$$L_{fe} = L_1 + L_2/v + L_3/v^2. \quad (16)$$

This ansatz is not as well-founded as (13), but it is justified by the results, as can be seen by Fig. 3, which is the velocity calibration curve of a set of all-oil measurements. It shows the velocity obtained by NMR $v_{NMR} = L_{fe}/T_E$ corresponding to (9) versus the velocity v_T obtained by the oil mass flow measured by the turbine at the oil input to the loop. These measurements have been done with the closed circular loop, as is usual for calibration measurements. It was the same set of measurements as shown in Figure 2. After this we opened the loop and did measurements of the velocity v and amplitude A_{00} with oil-nitrogen two-phase flow. Such measurements can only be done with the open-ended loop, because only then we can measure the mass flows of oil MF_1 (liquid) and nitrogen

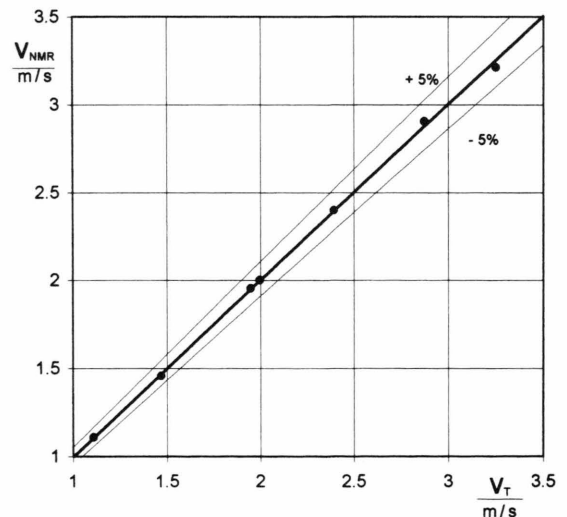


Fig. 3. Velocity v_{NMR} measured by NMR from EFC vs. velocity v_T measured by turbine in all-oil flow, serves as velocity calibration for oil-nitrogen flow.

MF_g (gas) before the mixing of both in a reasonable way. The oil-nitrogen mixture is then discharged after each measurement and the next measurement is done with a fresh mixture.

We always used fluctuation averaging by adding efflux curves together point by point. At all-oil flow (Fig. 3) we used 35 additions at low and up to 150 added curves at high velocities. At two-phase flow these numbers are 70 to 150. Such an adding of efflux curves improves on the signal-to-noise ratio S/N as well as on the signal-to-fluctuation ratio S/F caused by the flow. In our case, since we know the mass flow $MF_1 \equiv MF_T$ at the input into the loop, we can calculate the liquid fraction by the continuity equation. If v_T would be the velocity at all-oil flow and v_{NMR} the oil velocity at oil-nitrogen two-phase flow we obtain

$$\varepsilon_v = v_T / v_{NMR} \quad (17)$$

The comparison of ε_{NMR} , (15), and ε_v is given in Figure 4. All the values shown lie within $\pm 5\%$ of the exact value $\varepsilon_{NMR} = \varepsilon_v$ shown by the bold line. But at lower liquid fractions we have systematic deviations with $\varepsilon_{NMR} < \varepsilon_v$, which are probably due to two effects which take place particularly at annular flow and, since the heating oil has a viscosity of about 28 times that of water, they become more important with oil than with water flow. The critical velocity, which corresponds to the critical Reynold's number, amounts to

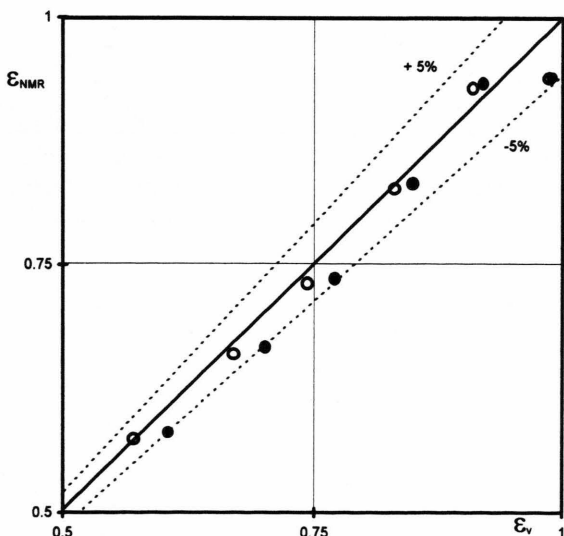


Fig. 4. Liquid fraction ε_{NMR} obtained from $(A_{00}/T_E)_{2p}$ in oil-nitrogen two-phase flow vs. ε_v obtained from the velocity v_{NMR} . Open circles are corrected values (see text).

about 6 cm/s for water and to about 160 cm/s for heating oil in our loop tube. In annular flow with oil the mixing of the spins due to turbulence of the flow during the polarization time t_p is therefore much weaker than in the case of water. We could not calculate this mixing effect, because we could not make calibration measurements with annular flow. That would have meant using two concentric loop tubes with the correct diameter ratio and with the oil flowing between the inner and the outer tube only. The result of this lack of mixing is, that the slower protons have a longer polarization time t_p and hence a larger amplitude than the fast ones. The efflux time distribution, which we use for the calculation of the velocity, is therefore shifted to longer efflux times T_E , and hence the velocity is given too small a value. The result is that ε_v comes out too large as compared with ε_{NMR} , which is exactly what we observe in Figure 4. This effect could be made smaller and the measurements therefore improved if we could install a long polarizing magnet before our measuring magnet. The polarizing field B_p does not need to be very large, since the NMR signals are large anyway, nor does it need a good homogeneity. But it is absolutely necessary that it has a sufficient physical length along the loop tube in order to obtain a long polarization time during which all the spins are completely mixed and hence would all be polarized in the same way. For our loop the length of the polarizing magnet should at least be 2 m.

A second disturbing effect is the inhomogeneity of the B_1 field, because in annular flow all the oil is near the wall of the tube, where B_1 is smaller than in the center, where the gas is flowing. The average efflux time and velocity of the oil are thus averaged somewhat differently at all-liquid and at liquid-gas flow. The remedy for this effect would be to enlarge the RF coil diameter. As B_1 in our case is by about 10% smaller at the tube wall than in the center, it would be only 0.6% smaller if we enlarged the diameter of the RF coil by 1.4 [5]. This would lower the signal and the signal-to-noise ratio by a factor of two. But this is not a serious problem because the NMR signals from such large coils are very large indeed. The accuracy of the measurement is not determined by the signal-to-noise ratio S/N but rather by the signal-to-fluctuation ratio S/F due to the fluctuations of the flow.

Since the systematic deviations shown in Fig. 4 are only about -5% we can correct them by an additional table in our computer program, and the result

Table 1. Results of two-phase flow measurements.

| | | | | | | |
|---|-------|-------|-------|-------|-------|-------|
| $\vartheta/^{\circ}\text{C}$ | 21.3 | 21.5 | 21.5 | 21.6 | 21.6 | 21.8 |
| $p_{\text{abs}}/\text{bar}$ | 3.2 | 2.9 | 2.7 | 2.6 | 2.4 | 2.3 |
| $\text{MF}_l/(\text{l/min})$ | 158 | 160 | 161 | 161.5 | 163 | 163.5 |
| $\text{MF}_g/(\text{l/min})$ | 253.4 | 117.9 | 84.7 | 61.3 | 36.4 | 17.0 |
| liquid $\varepsilon_{\text{loop}}$ | 0.384 | 0.576 | 0.655 | 0.725 | 0.817 | 0.906 |
| fractions ε_v | 0.604 | 0.702 | 0.770 | 0.849 | 0.920 | 0.990 |
| ε_{NMR} | 0.579 | 0.666 | 0.736 | 0.832 | 0.934 | 0.939 |
| $v_{\text{NMR}}/(\text{m/s})$ | 3.15 | 2.74 | 2.52 | 2.29 | 2.13 | 1.99 |
| $\text{MF}_{\text{NMR}}/(\text{l/min})$ | 151.4 | 151.9 | 154.0 | 158.3 | 165.5 | 155.1 |
| $\text{MF}_{\text{NMR}}/\text{MF}_l$ | 0.96 | 0.95 | 0.96 | 0.98 | 1.02 | 0.95 |

Values of liquid phase (oil)

| | | | | | | |
|---|-------|-------|-------|-------|-------|-------|
| liquid ε_v | 0.570 | 0.671 | 0.744 | 0.830 | 0.909 | 0.988 |
| fractions ε_{NMR} | 0.572 | 0.659 | 0.730 | 0.827 | 0.930 | 0.938 |
| $v_{\text{NMR}}/(\text{m/s})$ | 3.34 | 2.87 | 2.61 | 2.34 | 2.16 | 1.99 |
| $\text{MF}_{\text{NMR}}/(\text{l/min})$ | 158.8 | 157.2 | 158.4 | 160.9 | 167.0 | 155.2 |
| $\text{MF}_{\text{NMR}}/\text{MF}_l$ | 1.01 | 0.98 | 0.98 | 1.00 | 1.02 | 0.95 |

Corrected values of liquid phase (see text)

| | | | | | | |
|----------------------|---------------|---------------|---------------|---------------|---------------|---------------|
| ε_g | 0.43 | 0.34 | 0.27 | 0.17 | 0.07 | 0.06 |
| | ± 0.03 | ± 0.03 | ± 0.04 | ± 0.04 | ± 0.05 | ± 0.05 |
| $v_g/(\text{m/s})$ | 7.1 ± 0.5 | 4.2 ± 0.4 | 3.8 ± 0.6 | 4.3 ± 1.1 | 6.3 ± 7.4 | 3.3 ± 5.8 |
| v_g/v_{NMR} | 2.1 ± 0.2 | 1.4 ± 0.2 | 1.4 ± 0.2 | 1.8 ± 0.5 | 2.9 ± 3.4 | 1.7 ± 2.9 |

Calculated values of gas phase (nitrogen)

of this procedure is also shown in Fig. 4, where we have used no correction of the all-oil flow and about +6% for the velocity at low ε_v with linear interpolation in between. The corrected values are the open circles. Thus the overall accuracy of ε_{NMR} seems now even better than $\pm 5\%$.

Our results of measurements in two-phase flow are summarised in Table 1. The first two lines give the temperature ϑ in $^{\circ}\text{C}$ and the pressure p in bar abs at the measuring section of the loop. The next lines give the liquid mass flow MF_l in l/min measured by the turbine and the gas mass flow MF_g also in l/min measured by the MKS type 558 A mass flow meter before the mixing of both. There follow three liquid fractions $\varepsilon_{\text{loop}}$, ε_v , and ε_{NMR} as described in the text. Then we give the liquid velocity v_{NMR} and the mass flow obtained by v_{NMR} and ε_{NMR} . The last line of this first part of the table shows the ratio $\text{MF}_{\text{NMR}}/\text{MF}_l$, which gives directly the accuracy of the NMR measurement. The next part of the table shows the corrected values of the last five lines as described in the text. The correction is done at the velocity v_{NMR} , therefore ε_v is changed accordingly but ε_{NMR} changes only slightly. At the end of the table we give calculated values of the gas flow. The errors given correspond to $\pm 5\%$ error in ε_{NMR} . At

low liquid fractions the gas flows considerably faster than the oil and we have a slip in the order of two (last line of Table 1). At higher ε_{NMR} the gas fraction ε_g becomes very inaccurate because it has the same absolute error as the liquid fraction. Correspondingly we get large errors in the gas velocity and in the slip. The values and errors given here are certainly consistent with the assumption of no slip at these high liquid fractions.

Conclusions

We could show that the NMR mass flow measurement method developed in this laboratory can be applied to oil-nitrogen two-phase flow. In order to avoid unsuitable spin-lattice relaxation time corrections, we developed an approach via some constants due to the power series of $1 - \exp(-t_p/T_1)$, which works very well. We used time-averaging of the NMR signals in order to measure the average liquid mass flow in oil-nitrogen two-phase flow. This liquid mass flow shows a systematic deviation of -5% at low liquid fractions. This is due to insufficient mixing of the nuclear spins during the polarization period of the measurement and to the inhomogeneity of the B_1 RF field. It can be accounted for by a correction data base in the evaluation program of the spectrometer computer. The final overall accuracy of the NMR oil mass flow thus obtained is better than $\pm 5\%$.

Acknowledgements

The authors wish to thank Mrs. E. Dilger for her very careful and patient typing of the manuscript, which had been checked by Dr. S. Morris. Messrs. E. Malgarini and B. Paracchini helped with the measurements.

Nomenclature

| | |
|----------------------------|---|
| A_0 | maximum measured amplitude at beginning of an echo sequence, (10) |
| A_{00} | same amplitude normalized to attenuation 0 db, (10) |
| $(A_{00}/T_E)_{\text{AL}}$ | maximum value of A_{00}/T_E corresponding to all-oil flow, (13) |
| $(A_{00}/T_E)_{2p}$ | value of A_{00}/T_E at two-phase flow |
| A_1, A_2, A_3 | polynomial constants of $A_{00}/T_E(1/v)$, (13) |
| AT | attenuation at receiver input |
| B_0 | static magnetic field for NMR |
| B_p | static magnetic field for polarization |

| | | | |
|-----------------|--|-----------------------|--|
| B_{RF} | magnetic RF field | S/N | signal-to-noise ratio |
| B_1 | half the amplitude of B_{RF} | S/F | signal-to-fluctuation ratio |
| EFC | efflux curve, (1), (6) and (10) | T_1 | spin-lattice relaxation time, (1) |
| I | nuclear spin | T_2 | spin-spin relaxation time, (1) |
| ISC | iso-speed curve, (5) and (6) | T_E | efflux time, (1), (4), (8), and (9) |
| L_c | length of RF coil, (4) | $\langle T_E \rangle$ | average efflux time, (6) and (8) |
| L_{fe} | effective length of B_1 field, (9) | T_{Ei} | efflux time of spin group i |
| L_1, L_2, L_3 | polynomial constants of $L_{fe}(1/v)$, (16) | t_p | polarization time, (1) |
| M | nuclear paramagnetic magnetization parallel to B_0 | v | velocity, used also for mean velocity obtained by EFC, (9) |
| M_0 | thermal equilibrium value of M , (2) | $\langle v \rangle$ | average velocity, (9) |
| MF | gas mass flow | v_i | velocity of spin group i |
| MF_1^g | liquid mass flow | v_{NMR} | velocity determined by NMR |
| MF_T | liquid mass flow determined by turbine flow meter | v_T | velocity determined by turbine flow meter |
| MF_{NMR} | liquid mass flow determined by NMR | γ | magnetogyroscopic ratio, (3) |
| $m(t)$ | nuclear magnetization perpendicular to B_0 , (1), (4), (5), and (10) | ε | any fraction of bulk matter |
| m_0 | maximum value of $m(t)$, (4), (5), (6), and (7) | ε_g | gas (void) fraction |
| m_{0i} | same for all the spins of velocity v_i , (6), (7), and (8) | ε_l | liquid fraction |
| p | pressure in bar abs. at test section | ε_{loop} | liquid fraction obtained by loop input data |
| RF | radio frequency | ε_{NMR} | liquid fraction obtained by $(A_{00}/T_E)_{2p}$, (15) |
| | | ε_v | liquid fraction obtained by v_{NMR} , (17) |
| | | ϑ | temperature in C at test section |
| | | χ_0 | static nuclear paramagnetic susceptibility, (3) |

[1] A. Caprihan and E. Fukushima, Flow measurements by NMR, Physics Reports **198**, 195 (1990).

[2] G. J. Krüger, J. Haupt, and R. Weiss, A Nuclear Magnetic Resonance Method for the Investigation of Two-Phase Flow, in: Measuring Techniques in Gas-Liquid Two-Phase Flows, IUTAM Symposium Nancy, France (1983) 435–454, J. M. Delhay and G. Cognet, Eds., Springer, Berlin 1984.

[3] A. Abragam, The Principles of Nuclear Magnetism, 2nd Edition, Oxford University Press (1962).

[4] S. Meiboom and D. Gill, Rev. Sci. Instrum. **29**, 688 (1958).

[5] G. J. Krüger, Coil for the production of homogeneous magnetic fields, 16 pages, US Patent 423 1008 (1980).